NASA TECHNICAL TRANSLATION NASA TT F -15,110

A COMPARISON BETWEEN MEASURED TRANSMISSION AND EMISSION SPECTRA AND CALCULATED SPECTRA IN THE 9.6 μm REGION OF OZONE

D. Marzoch

Translation of "Ein Vergleich gemessener Transmissions- und Emisionsspektren mit berechneten Spektren in der 9.6 μ-Bande des Ozons," Ludwig-Maximilians-Universitat, Munich (West Germany), Report MBFT-FBW-73-01, Jan. 1973, 52 pages

(NASA-TT-F-15110) A COMPARISON BETWEEN MEASURED TRANSMISSION AND EMISSION SPECTRA AND CALCULATED SPECTRA IN THE 9.6 MICRON REGION OF OZONE (Kanner (Leo) Associates) ~~36~~ 39 p HC $4.00 CSCL 04A

N73-31356

Unclas G3/13 14518

NATIONAL AERONAUTICS AND SPACE ADMINISTRATION
WASHINGTON, D.C. 20546 SEPTEMBER 1973

STANDARD TITLE PAGE

1. Report No.	2. Government Accession No.	3. Recipient's Catalog No.
NASA TT F-15,110		

4. Title and Subtitle	5. Report Date
A COMPARISON BETWEEN MEASURED TRANSMISSION AND EMISSION SPECTRA AND CALCULATED SPECTRA IN THE 9.6 μm REGION OF OZONE	September 1973
	6. Performing Organization Code

7. Author(s)	8. Performing Organization Report No.
D. Marzoch	10. Work Unit No.

9. Performing Organization Name and Address	11. Contract or Grant No.
Leo Kanner Associates Redwood City, California 94063	NASw-2481
	13. Type of Report and Period Covered
	Translation

12. Sponsoring Agency Name and Address	14. Sponsoring Agency Code
National Aeronautics and Space Administration, Washington, D.C. 20546	

15. Supplementary Notes

Translation of "Ein Vergleich gemessener Transmissions- und Emisionsspektren mit berechneten Spektren in der 9.6 μ-Bande des Ozons," Ludwig-Maximilians-Universitat, Munich (West Germany), Report BMFT-FBW-73-01, Jan. 1973, 52 pages.

16. Abstract

Measurements of the atmospheric transmission and emission are compared with the calculated spectra obtained from Clugh and Kneizys' theoretical line parameters. The comparison shows that the use of these line data recently fitted to laboratory measurements of McCaa and Shaw by Rest leads to incorrect results. Spectra computed with the latest releasted theoretical line data compare well with transmission measurements made from the ground. However, there remains a noticeable discrepancy in comparison with IRIS-spectra obtained from the US satellite Nimbus 3.

17. Key Words (Selected by Author(s))	18. Distribution Statement
	Unclassified-Unlimited

19. Security Classif. (of this report)	20. Security Classif. (of this page)	21. No. of Pages	22. Price
Unclassified	Unclassified	34	

Table of Contents

Table of Illustrations

List of Symbols

A_λ	Spectral measurement deviation of the actual transmission spectrum
A'_λ	Spectral measurement deviation of the measured tranmission spectrum
α	Half-width value
$B_\lambda(T)$	Spectral radiant flux density of reference emitters
c	Speed of light in a vacuum
D'_λ	The wavelength dependent on "transmission" of the spectrograph
g	Gravitational acceleration
h	Planck's constant
I_ν	Source function
k	Boltzmann's constant
k_ν	Spectral absorption coefficient
m	Mass
M	Molecular weight
N_ν	Spectral radiant flux density per wave number
ν	Wave number
p	Pressure
R_L	Gas constant of dry air
ρ	Density
S	Line intensity
T	Absolute temperature
τ_ν	Spectral transmission per wave number
u	Optical path
ζ	Zenith angle

A COMPARISON BETWEEN MEASURED TRANSMISSION AND EMISSION SPECTRA AND CALCULATED SPECTRA IN THE 9.6 μm REGION OF OZONE

D. Marzoch
Meteorological Institute, Ludwig-Maximilians-Universität, Munich

1. Introduction

/8*

The line spectra of the 9.6 μm band of ozone from Clough and Kneizys, 1965 [7] were compared with laboratory spectra from McCaa and Shaw, 1967 [17] in the thesis of Rest, 1968 [24]. They were corrected empirically to reproduce these ozone bands as accurately as possible by calculations carried out line by line with actual atmospheric data.

Comparisons of spectra calculated in this way with the corresponding measured spectra have been made previously only with the laboratory spectra of the entire band from McCaa and Shaw and with emission measurements in short spectral ranges by S. Agata, Jungfraujoch (Bolle, 1961) and Pallestine (Hanel, 1966). The results indicated very good agreement. However, it was desirable to compare more spectra with higher dispersion of the entire 9.6 μm band. The measurement prerequisites were given in 1969, because a heliospectrograph for transmission measurements was available in Maisach, and emission measurements were being carried out at the same time by the IRIS (infrared interferometer spectrometer) from the satellite Nimbus III.

Recently, comparisons between calculated and measured spectra in the range of 9-10 μm have been successfully carried out by Goldman et al., 1968 [10]. The spectra were calculated line by line, naturally taking the "hot bands" of ozone into consideration. The line data used here were later made available to the author from Selby and McClatchery, 1970 [18], so that another comparison was possible.

Another method for the calculation of the absorption spectra of IR bands is the statistical band model developed by Goldman and Kyle, 1968 [11, 12].

These lines or band models are interesting because, with their /9
help in comparing calculated and measured spectra, statements can be made about the line data of a particular gas. With more exact knowledge of the transmission function, the ozone content of the atmosphere can also be determined with greater certainty from satellite spectra by inversion methods (Prabhakara, 1970 [22]).

---

* Numbers in the margin indicate pagination in the foreign text.

2. Transmission Measurements in Maisach /10

2.1. Measurement Times in Maisach

The first transmission measurements of the measurement station Maisach, 35 km west of Munich at the Fürstenfeldbruck airport, were possible on May 22, 23, and 27, 1969. (A summary of these measurements is given in the appendix.) It was attempted to schedule the measuring periods for the late afternoon, when Nimbus III flew over central Europe and made emission measurements.

Of these three days, May 27 was especially good because the measuring location and time of the satellite and earth station came the closest then.

2.2. Measuring Equipment for the Transmission Measurements

The heliospectrograph for the transmission measurements in Maisach consists of a coelostat and a solidly constructed diffraction grating spectrograph (H. Grassl, P. Wendling, H.J. Bolle, 1969 [13]).

The sunlight passes from the plane mirror of the coelostat ($\varnothing$ 60 cm), which can be automatically directed by a sun-seeking device over several mirrors to the entrance slit of the spectrograph. The grating spectrograph is constructed on the principle of Czerny-Turner, the focal length of both spherical mirrors is 2 m, the Echelle grating is moved by a driving gear that is constructed to make the wavelength feed linear. A Golay detector was available to measure the intensity of the solar radiation. A reference emitter could be omitted, because the intensity of the incident solar radiation is very high at 10 µm, and no absolute measuring was done. The blackened surface of the chopper, which can be omitted at this wavelength, unlike the direct incident solar radiation, was sufficient as a reference point. /11

A spectral dispersion of 1 wave number was reached during the measurements by this spectrograph with a slit width of 4 mm.

2.3. Determination of the Transmission Characteristics of the Spectrograph

The spectrum produced by the spectrograph is changed by its characteristic transmission. This means

$$A'_\lambda = D'_\lambda \cdot A_\lambda . \qquad (2.1)$$

A'_λ is the experimental value of the measured spectrum at a definite wavelength, A_λ is the corresponding test value of the "true spectrum." $D'_\lambda = C \cdot D_\lambda$ is the wavelength dependence of the spectrograph transmission. A Nernst glower at a working temperature of approximately 1700°K was used to determined D'_λ, because the 56°C black body available at the time could not deliver enough energy to the spectrograph with a fully opened slit of 4 mm and a high dispersion of 1 cm^{-1}. In detail, the following processes were carried out: The 56°C black body was measured over the desired spectral range in another spectrograph with a lower dispersion, and then the "transmission curve" D'_λ of the spectrograph was determined by using the absorption tables. The graph is obtained from the following relations:

$$A'_\lambda = D'_\lambda \cdot [B_\lambda(T_1) - B_\lambda(T_2)]. \qquad (2.2)$$

$B_\lambda(T_1)$ is the spectral radiant flux density of the reference emitter, $B_\lambda(T_2)$ is the spectral radiant flux density of the comparison emitter. If the same measurement is carried out once more with the Nernst glower, the "true" intensity of the Nernst glower can be determined by using the transmission curve now known. Another measurement of the Nernst glower with the spectrograph that was used for the transmission measurements gives the needed transmission curve by comparison with the "true" Nernst glower curve. Naturally, only relative values can be obtained by this process. /12

It should also be noted that the Nernst glower showed no significant variations in intensity during a long measurement period and therefore could be used as a calibration source.

3. Emission Measurements from Nimbus III /13

3.1. The Nimbus III Satellite

Nimbus III was launched on April 14, 1969, and flies a nearly circular orbit of 600 nautical miles ($\approx$ 1100 km). The individual orbits cross the equator at intervals of 26° longitude. One orbit lasts 107 min, which corresponds to about 13 orbits per day [20, 21]. If a particular region of the earth is considered, from which measurements can be compared to those from the satellite, then these comparisons are possible 13 days a month at a geographical position within a range of ±4°. Poor weather conditions can reduce this number of days considerably, however.

The emission measurements of ozone in the 9.6 µm band were carried out in the IRIS experiment.

3.2. The IRIS Experiment

The IRIS experiment (infrared interferometer spectrometer) by R. Hanel and B. Conrath [14, 20, 21] began during the eighteenth orbit and ended measurements on July 22, 1969, during orbit 1332. The goal of this experiment was to obtain information about vertical temperature profiles, ozone, water vapor, emission of the earth's surface, and atmospheric gases in low concentrations (CH_4 and N_2O).

The instrument, a Michelson-infrared-interferometer spectrometer, measured the thermal emission spectrum of the earth in the region of 5-25 μm (= 2000 to 400 cm^{-1}) with a spectral dispersion of 5 wave numbers. It possessed a conical field of vision with a bevel angle of 8°, which corresonds to an area on the earth's surface with a diameter of about 150 km from an altitude of 1100 km.

From the spectral range of 5-25 μm, it was therefore easy to obtain the range that is significant for the emission of ozone, and /14
that could also be compared with the range of transmission measurements.

On May 27, 1969, Nimbus III flew over the region with the central point of Kempten approximately during the measuring time period in Maisach. Thus it was possible to compare emission and transmission measurements, and to join the emission and transmission programs for the calculations, since the same ozone, water vapor and pressure distribution were involved in both.

In Fig. 3.1, a section of the line of flight of Nimbus III on May 27, 1969 can be seen with the corresponding measurement regions. Figs. 3.2 to 3.4 show the cloudiness on May 26, May 27, and May 28, 1969, which was also measured from Nimbus III by the high resolution infrared radiometer (HRIR).

4. Calculation of the Transmission and Emission Spectra /15

4.1. Fundamental Equations of the IR Radiation Transmission

The fundamentals of the process used here to calculate the IR radiation transmission have already been discussed in Bolle, 1967 [4] and Rest, 1968 [24]. Therefore, only a brief summary of the equations essential for the determination of transmission and emission will be given.

The spectral radiant flux density is changed by the mass dm during its passage through an atmospheric layer because of absorption and emission. The absorption portion is given by

$$(dN_\nu)_a = -k_\nu N_\nu dm \qquad (4.1)$$

k_ν = absorption coefficient and the emission portion by

$$(dN_\nu)_e = +k_\nu I_\nu dm \qquad (4.2)$$

I_ν = source function. If the increment of the optical path $k_\nu dm$ is replaced by du:

$$du = -k_\nu dm, \qquad (4.3)$$

then the total change of the radiant flux density is obtained from (4.2) and (4.4):

$$dN_\nu = (dN_\nu)_a + (dN_\nu)_e = N_\nu du - I_\nu du. \qquad (4.4)$$

$I_\nu(u)$, the source function is given by the Planck function for $p > 0.034$

$$B_\nu(T) = \frac{2h\nu^3 c}{e^{h\nu c/kT}-1} . \qquad (4.5)$$

The integration of (4.1) applies to the calculation of the pure absorption:

$$\frac{N_\nu}{N_{\nu_0}} = \exp\int -k_\nu dm , \qquad (4.6)$$ /16

or, since N_ν/N_{ν_0} is labeled as transmission τ_ν:

$$\tau_\nu = \exp\int -k_\nu dm. \qquad (4.7)$$

To calculate the transmission toward the sun in the 9.6 μm band of ozone, it is sufficient to use Eq. (4.7) without considering the influence of the characteristic radiation of the atmosphere. The relation of the sun's radiant flux density, ~5000°K, to the atmosphere, about 280°K, lies in the order of magnitude 1000 to 1.

The contribution of the emission can be ignored for this reason, because only portions of the sun contributed to the measuring signal of the heliospectrograph that was used. If the emission is nevertheless taken into consideration, then Eq. (4.4) is applicable. If both sides are multiplied by e^{-u} and the transmission function $\tau_\nu(u) = e^{-u}$ is introduced, the result is

$$d(N_\nu \tau_\nu) = I_\nu d\tau_\nu \,. \tag{4.8}$$

If this equation is integrated over the optical path with the initial point u_1 and the end point u_2, the complete radiation transmission equation is obtained:

$$N_\nu(u_1) = N_\nu(u_2)\tau_\nu(u_2,u_1) - \int_{u_1}^{u_2} I_\nu(u)d\tau_\nu(u) \,. \tag{4.9}$$

since $\tau_\nu(u_1, u_1) = 1$. For the comparison with satellite measurements, Eq. (4.9) should be reformed correspondingly, i.e. the radiation that disperses into outer space is considered. The optical path length is replaced by the altitude above sea level. The relation between the two is

$$du = k_\nu(h)\rho(h)dh, \quad (\rho = \text{ozone density}) \tag{4.10}$$

since the relative air mass is equal to 1 in this case. If the altitude from the earth's surface is labeled h_0 and the atmospheric circumference h_∞, and $N_\nu(u_2)$ is replaced by the source function $I_{\nu,B}(\zeta)$, which is the radiant flux density emitted from the earth under the zenith angle ζ, then the equation for the radiation dispersing into outer space is /17

$$N_\nu(h_\infty,\zeta) = I_{\nu,B}(\zeta)\tau_\nu(h_0,h_\infty) - \int_{h_0}^{h_\infty} I_\nu(h)d\tau_\nu(h). \tag{4.11}$$

In applications to the atmosphere it is better to integrate altitude rather than pressure. The relation between them is easily determined with the hydrostatic fundamental equation and the ideal gas law. Taking (4.3) and (4.10) into consideration, (4.7) therefore appears as

$$\tau_\nu = \exp\left[-\int k_\nu \frac{\rho R_L T}{\mathcal{G}p}\, dp\right] . \quad (\rho = \text{ozone density}) \tag{4.12}$$

4.2. Calculation of the Transmission from Line Data

The simple Lorentz profile is used to calculate the O_3 transmission from line data:

$$k_\nu = \frac{S}{\pi} \frac{1}{(\nu-\nu_0)^2 + \alpha^2} \quad . \tag{4.13}$$

The half-width value is calculated from:

$$\alpha = \alpha_0 \frac{p}{p_0}\sqrt{\frac{T_0}{T}} \quad . \tag{4.14}$$

α_0 is the half-width value at p_0 and T_0, and has the constant value 0.089 cm^{-1} for the transmission calculations of ozone. This value applieds at NTP. Since calculations are made up to a pressure of 0.1 mbar in this program, the Doppler effect must be considered in the distribution of the spectral lines (Armstrong, 1966 [1]). This is taken into consideration in the present calculation program if the relations $\alpha/\alpha_D < 5$ and $(\nu - \nu_0)/\alpha_D < 5$ are realized. The line distribution caused by the Doppler effect is described by α_D:

$$\alpha_D = 3{,}58 \cdot 10^{-7}\sqrt{\frac{T}{M}}\ \nu_0 \tag{4.15}$$

(M = molecular weight). As calculations from Kunde, 1967 [15] have shown, the preceding conditions are sufficient to describe the influence of the Doppler effect. /18

The line intensity S or integral absorption is still lacking as an additional dimension for the determination of the absorption coefficient.

$$S = \int_{-\infty}^{+\infty} k_\nu d\nu. \tag{4.16}$$

The temperature dependence of the line intensity is:

$$S = S_0 \Phi(T) \quad , \tag{4.17}$$

while S_0 gives the line intensity at the reference temperature T_0

in degrees Kelvin. If it is desired to give S in $cm^{-2} \cdot atm^{-1}$, as in the case of ozone, then $S = S_0(T_0/T)\Phi(T)$. $\Phi(T)$ is a temperature function and is summarized in the following way:

$$\Phi(T)=\left(\frac{T_0}{T}\right)^r \exp[-1{,}4388\nu''(T^{-1} - T_0^{-1})]\frac{1 - \exp\frac{-1{,}4388}{T}\nu_0}{1 - \exp\frac{-1{,}4388}{T_0}\nu_0} \qquad (4.18)$$

ν_0 is the line center, $\nu'' = E''/hc$ is the wave number that would correspond to a transition from energy level E" -- the lower transition level -- to zero. r depends upon the type of molecule, and, for example, is 1.5 for O_3 and H_2O. Now the transmission of separate lines can be calculated from Eqs. (4.13), (4.14), (4.17) and (4.18) with Eq. (4.7).

In the calculation program used here, a variable step size is chosen which begins at the line center with the minimum step size $\Delta\nu = 0.001\ cm^{-1}$ and is raised to the maximum step size $\Delta\nu = 0.01\ cm^{-1}$ by doubling. If this value is reached, the step size remains constant. The point at which a decreasing step size begins again is always located so that the minimum step size ends exactly at the next line center. /19

The calculation process is carried out for the gases O_3, H_2O and CO_2 of separate atmospheric layers, and the transmission values obtained are joined according to the relation $\tau_{\nu total} = \tau_{\nu O_3} \cdot \tau_{\nu H_2O} \cdot \tau_{\nu CO_2}$.

The line intensities used for the calculation of the entire spectrum from 950-1100 cm^{-1} were previously the line intensities from Clough and Kneizys [7], corrected by Rest [24]. Later, the spectral region from 1030-1035 cm^{-1} could also be calculated with the new line data from Selby and McClatchey [18].

4.3. Atmospheric Model

To calculate the transmission through the atmosphere and the emission toward outer space and the earth, it is necessary to divide the atmosphere into layers for the integration. The division of layers in the program used here is arranged to allow consideration of marked pressure values from radiosonde ascents. The essential part of this program for the observer, however, is the fine divisions of layers. The radiant intensities which are measured in the air or on the ground are most affected by the layers directly bordering on them. This influence is taken into account by the fine division of layers.

For the calculation of the tranmission and emission spectra from May 27, 1969, the values of the radiosonde ascent Munich-Riem at 12:00 GMT [Greenwich Mean Time] were given for the pressure,

temperature, and water vapor distribution in the layer model. The measurement values from Maisach were used for the ground values (Fig. 4.1). The ozone distribution comes from the measurements from Hohenpeissenberg on May 28, 1969, 7:41 Central European Time (Fig. 4.2). The lacking distributions were completed up to 0.1 mbar according to the table values of Bolle, 1967 [4], which has as a basis the US Standard Atmospheres 1962 and recommended water vapor /20
and ozone distributions from the Handbook of Geophysics. Table values on the zenith angle of the sun dependent on the measuring time are available for Maisach (Quenzel [23]).

5. Evaluation of the Transmission Measurements /21

The best "window" is located in the measured spectral region from 950-1100 cm^{-1}, thus the spectral region of the least absorption at 986 cm^{-1} (= 10, 14 µm) (Farmer, Key, 1965 [9], Migeotte et al., 1956 [19]).

To correct the influence of the continuum absorption, and to obtain the equivalent measurement deviation of the extraterrestrial solar spectrum, it is necessary to carry out measurements of differing zenith angles of the sun in the window range to extrapolate zero from the air mass. This was impossible due to poor weather conditions. A correction was made with the water vapor continuum, so that this measurement deviation could be determined. This applies to the tranmission in the window:

$$\tau_F = \exp(-k_{\nu,o} \frac{p_e}{p_o} \cdot m_{H_2O}). \qquad (5.1)$$

$k_{\nu,0}$ is the absorption coefficient for the water vapor continuum and is 0.09 $g^{-1}cm^2$ at 10.1 µm (Bolle, 1967 [4]). p_e is the effective pressure for H_2O (= 775 mb), p_0 = 1013 mbar, m_{H_2O} gives the water vapor mass in gcm^{-2}. The extraterrestrial measurement deviation of the solar spectrum A_ν is obtained from:

$$A_\nu = \frac{A'_{\nu\ gem}}{\tau_F} . \qquad (5.2)$$

$A_{\nu\ gem}$ is the measurement deflection of the measuring intensity in the window. The black body curve of the sun was set through this point, the measurement deviation A_ν at 986 cm^{-1}, with a radiation temperature of 5036°K. It acted as an envelope of the spectrum (Saiedy and Goody, 1959 [16]), so that the transmission τ_ν could be calculated at any desired point. The value for the sun's radiation temperature from Labs, 1968 [16], 5145°K at 10 µm was not used

because it was discovered only after the completion of the evaluation. The use of 5036°K instead of 5145°K results in a relative error of -0.2% with this evaluation procedure. /22

The influence of extinction by the dry aerosol in the range of 10 µm can be disregarded during the evaluation of the measurements. But at relative humidities over 75%, the influence of the expanding aerosol would have to be considered according to Carlon, 1970 [6]. During all of the measurements in Maisach, the relative humidity remained below this value in the lower atmospheric layers, which contain the most aerosol.

6. Comparison Between Calculated and Measured Spectra /23

6.1. Transmission Spectra

The comparison between calculated and measured transmission spectra was made on spectrum 27/1 from May 27, 1969 for O_3 alone as well as for $O_3 + H_2O + CO_2$ (see Fig. 3 in the appendix). H_2O and CO_2 could be corrected in the measured transmission spectra with the help of the calculated transmission values of both gases. Since $\tau_{\nu\,ges} = \tau_{\nu O_3} \cdot \tau_{\nu H_2O} \cdot \tau_{\nu O_2}$, $\tau_{\nu O_3}$ is easily calculated. For the comparison with the measured spectra, the calculated spectra were flattened with a triangular slit function, which had a half-width value of 1 cm^{-1} for the transmission spectra and 5 cm^{-1} for the emission spectra. In Figs. 6.1 and 6.2, respectively, the two curves are contrasted.

As both illustrations show, the course of the spectra is reproduced very effectively by the calculation. Greater deviations from the measured transmission values appear in the range 980-1010 cm^{-1} (relative error -6.1%, up to -15% for single wave numbers). However, the integral absorptions over the entire band do not deviate from each other.

In the range 1030-1035 cm^{-1}, calculations could be made again with new uncorrected line data and the same ozone distribution. Due to the large number of these new line data (an increase in the number of lines from 3500 to 10,000), the calculations for a larger spectral region were too demanding.

The mentioned range was therefore chosen, to determine whether the influence of the overlapping of Q and P branches on the transmission can be reproduced better with the new line data. As Fig. 6.2 shows, if an improvement can actually be determined, the deviation of the transmission of the calculated spectral range from that of the measured range will be decreased by 40%. /24

To determine how the transmission of the entire band changes when the new line data are used, one of the transmission spectra for p, T = const given by Rest was calculated, employing the corrected Clouch and Kneizys data, with the new O_3 line intensities.

In addition, one was chosen that had an O_3 mass of 0.41 atm-cm at a pressure of p = 66.6 mbar. Fig. 6.3 compares the "laboratory spectra" calculated with corrected and new line data. The same discrepancies appear in the same spectral ranges as the one in the spectra from Maisach. This is especially noticeable in the range from 1050-1065 cm^{-1}, where the transmission values obtained with the corrected line data are too high. Thus, there is reason for the conjecture that the laboratory spectra of McCaa and Shaw, to which the line data used by Rest was adapted, were inaccurate. The result is correspondingly inaccurate line intensities.

In Fig. 6.2, if the relation of the integral measurement and calculation transmissions is constructed for the spectral regions 980-1000 cm^{-1} and 1050-1065 cm^{-1}, and compared in Fig. 6.3 with the relation of calculated integral transmissions with new and corrected line data for the same spectral ranges, these values agree within a 3% deviation. This confirms the conjecture of incorrect line data, and it also shows that the spectra can be reproduced effectively in these ranges with the new data.

In Fig. 6.4, spectra calculated with uncorrected line intensities from Clough and Kneizys and new line data (m = 0.41 atm-cm, p = 66.6 mbar) are compared again to show the essential changes in the transmission values. /25

6.2. Emission Spectra

IRIS measurements from Nimbus III from May 27, 1969, 10:00 GMT were available, as already mentioned in Chapter 3, for the comparison of emission measurements. The spectrum that was used represents the middle circular measuring range with the center point 47.8°N and 10°C in Fig. 3.1. The pressure, temperature, and water vapor distribution were again obtained from the radiosonde ascent Munich-Riem at 12:00 GMT on the same day; the ozone distribution was obtained from Hohenpeissenberg on May 28, 1969. Statements about the ozone variation between Hohenpeissenberg (Attmannspacher, 1969 [2, 26]), Faverne, and Arosa (Dütsch, 1970 [8]) can be obtained from Table 7.1 and Figs. 4 and 5 in the appendix.

Fig. 6.5 shows the comparison of the calculated and measured spectrum (lower and upper curve). The course of the spectrum is reproduced well here too, except that the calculated curve has lower values with respect to the measured curve than the corresponding curves of the transmission spectra. The reason for this may lie in varying ground temperatures, as the assumptions of 293.5°K and 289°K show in Fig. 6.5. The displacement by 1 wave number in the center can be attributed to the satellite data, because it does not appear in the transmissions, although the same calculation process is used. 19°C is given in the daily weather reports for the ground temperature on May 27, 1969, 13:00 Central European Time in Kempten, which was located in the measurement

area. The deviation in temperature values should therefore be considered a consequence of regional and temporal differences in measurements.

To investigate more closely the assumption of differing ground temperatures for the calculated and measured emission spectrum, the following evaluation is carried out, which is obtained by adaptation of the calculated to the measured spectrum.

The following relations apply to the radiant flux density measured by the satellite: /26

$$A_\nu = B_\nu(T_1)\cdot\tau'_\nu + \text{Emission d. Atm.} \qquad (6.1)$$

$$A'_\nu = B_\nu(T_2)\cdot\tau'_\nu + \quad -\,"\,- \qquad (6.2)$$

$B_\nu(T_1)$ and $B_\nu(T_2)$ give the radiant flux density of the ground temperatures $T_1 = 293.5°K$ and $T_2 = 289°K$. If (6.2) is withdrawn from (6.1), then:

$$A_\nu - A'_\nu = [B_\nu(T_1) - B_\nu(T_2)]\cdot\tau'_\nu \text{ und} \qquad (6.3)$$

$$A_\nu = A'_\nu + [B_\nu(T_1) - B_\nu(T_2)]\cdot\tau'_\nu . \qquad (6.4)$$

The middle curve in Fig. 6.5 shows the calculated spectrum adapted to the measured spectrum by Eq. (6.4), when the necessary calculated tranmission values τ_ν from Fig. 6.1 are used. It is evident that a significant improvement in the calculated intensities actually appears. An indication of higher values in the spectral range from 1050 to 1060 cm^{-1} can also be determined here, as in the transmission measurements (Figs. 6.1 and 6.2). In Fig. 6.5 the relative errors of the adapted curves to the measured curves are in the region 990-1010 cm^{-1}, -2.3% ; 1050-1060, cm^{-1} +2.6%; and 990-1065 cm^{-1}, -2.5% (entire band).

In Fig. 6.6 an estimation of how the emission spectrum would be distributed if it were calculated with new line intensities is shown. This estimation can be carried out according to formula (6.4), if the following is changed:

$$A_\nu = A'_\nu + (\tau_\nu - \tau'_\nu)\cdot B_\nu(T). \qquad (6.5)$$

τ_ν is the measured transmission of Fig. 6.1, τ'_ν is the calculated transmission, and $B_\nu(T)$ is the spectral radiant flux density for $T = 293.5°K$. Apparently, the use of the new line data would bring /27 no improvement according to this estimation. So the relative errors are now in the range 990-1010 cm^{-1}, +3.8%; 1050-1060 cm^{-1}, -9.2%; and 990-1065 cm^{-1}, -2.0% (entire band). Of course, the displacment of the wave number has not yet been considered. Therefore, all three curves are again superimposed in Fig. 6.7, so that the centers coincide. For the relative errors relative to the measured curves, the following values are determined:

	Corrected line data	New line data
1050-1060 cm^{-1}	+6.5% relative error	-5.9% relative error
990-1010 cm^{-1}	-4.4% " "	+2.4% " "
990-1065 cm^{-1}	-2.9% " "	-2.5% " "

It is evident that the calculations with new line data also make a better reproduction of the measured values possible, so that the result of the estimations for the transmission spectra evaluated in this work is confirmed.

It was possible to calculate the emission through the atmosphere with new line intensities for the spectral range 1030-1035 cm^{-1}. The comparison between this and emissions calculated with old and new line intensities can be seen in Fig. 6.8. Because of the small spectral range, a dispersion of 1 wave number had to be used. Thus, direct comparisons with the measurement and calculation of the dispersion of 5 wave numbers is scarcely possible. However, it is evident from the comparison in Figs. 6.5 and 6.8 that the emission values calculated with new data are lower than the values calculated with old data, so that the evaluations carried out previously are also confirmed here.

7. Sources of Error /28

Since the pressure, temperature and water vapor distribution could not be obtained at the time of measurement to calculate the spectra, with the exception of the ground values measured in Maisach, the radiosonde ascents Munich-Riem at 12:00 GMT had to be employed. Evidently, several sources of error that are difficult to estimate could appear, especially in relation to changes in water vapor content and temperature in higher atmospheric layers. The case of the ozone distribution is also unfavorable. The distribution on May 28, 1969 from Hohenpeissenberg, as the nearest measurement location, had to be accepted for May 27, 1969, and it is evident from comparisons with total ozone measurements from Arosa and Hohenpeissenberg in Table 7.1, that the total ozone content was higher on May 27, 1969 than on May 28, 1969 by 5.6%.

TABLE 7.1. MEASURED TOTAL OZONE CONTENT IN matm-cm

	Hohenpeissenberg	Arosa
20 May 1969	396	373
21 May 1969	361	349
22 May 1969	371	349
23 May 1969	339	337
24 May 1969	355	346
27 May 1969	357	352
28 May 1969	337	336
29 May 1969	384	371

As the table and the ozone profiles of Figs. 4 and 5 in the appendix show, regional differences for the ranges appearing here -- which applies to May 27 and May 28 -- can be disregarded. Since this data was first known to the author during the course of this calculations, a correction could not be made.

During the evaluation of the transmission spectra, it was discovered that the measurement values in the "window" were not correlated with the zenith angle of the sun, but fluctuated irregularly, which probably can be attributed to weak cirrus clouds. The relative error of the mean value from measurements of nine different angles of the zenith is ±5%. Nevertheless, these fluctuations have no significant negative effects in the course of further evaluations with the solar curve and the water vapor continuum. /29

8. Conclusion /30

As the evaluations and estimations in this work show, the following statements may be made:

The adaptation of the line data from Clough and Kneizys to laboratory spectra from McCaa and Shaw by Rest produced incorrect values, since the laboratory measurements were obviously defective.

This can be determined very definitely in the spectral regions 980-1000 cm^{-1}, 1030-1035 cm^{-1} and 1050-1065 cm^{-1}. It has also been proved that measured spectra can be reproduced best by calculations employing the new line data of Selby and McClatchery. The large discrepancies that occurred with the Rest data in the spectral ranges studied here can be reduced with the new data. This applies particularly to the calculated transmission spectra, while a deterioration occurs with the calculated emission spectra in the spectral region from 1030-1040 cm^{-1}. Defective data material for the emission measurements is a possibility, as the displacement by 1 wave number in the comparisons between calculations and measurements indicates. Measurement inaccuracies that appeared in the

transmission measurements in Maisach would not reduce the continuing discrepancies by more than 1%.

Naturally, it would make a better statement if the new line data were given another examination with the entire 9.6 μm band. However, this should take place with atmospheric transmission spectra, not with laboratory spectra, since ozone is very difficult to handle in the laboratory. But the calculation of atmospheric transmission spectra with new data means a monstrous expenditures for computation. To calculate the absorption coefficients k_ν and the corner integrals for O_3 in the spectral region 1030-1035 cm^{-1} with new line data, a pure computing time of 27 hours was required in Offenbach on the CDC 3800. That would correspond /31 to a computing time of 2 to 3 hours on the IBM in Garching. For this reason, it seems more sensible to change to band models, as they were developed by Goldmann, for example. The parameters of this statistical band model were determined for intervals of $\Delta\nu = 5$ cm^{-1} and for three representative temperatures. Therefore, a meaningful comparison with the atmospheric transmission spectra of 1 wave number dispersion is first possible, when the intervals are diminished correspondingly and the parameters are calculated for more temperature.

The voluminous calculations were carried out on the CDC 3800 of the German Weather Service in Offenbach. Mr. W. Attmannspacher and Mr. H. U. Dütsch are thanked for sending the ozone profiles, and Mr. R. Hanel and Mr. B. C. Conrath are thanked for sending the IRIS measurements. The corrected line data were placed at the disposal of the author before publication by Mr. J. E. Selby and Mr. R. A. McClatchey. Miss B. Pornitz must be thanked for the execution of the calculations. The work was supported by the Federal Ministry for Education and Science as a research project of WRK 214.

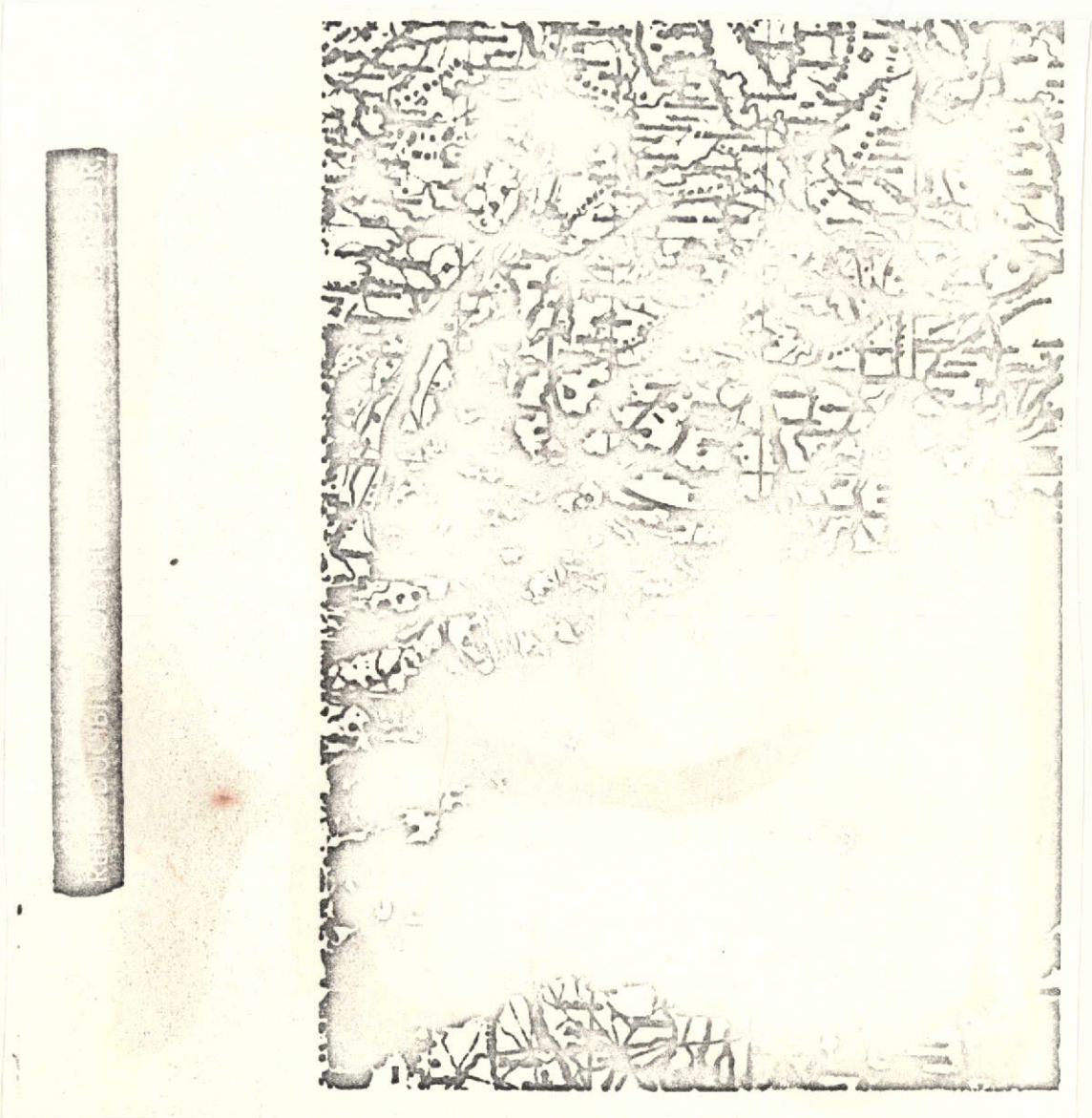

Fig. 3.1. Measurement ranges of IRIS on May 27, 1969, 10:03:21 to 10:03:53 GMT. Time interval per measurement 16 sec, flight direction SSE to NNW.

/34

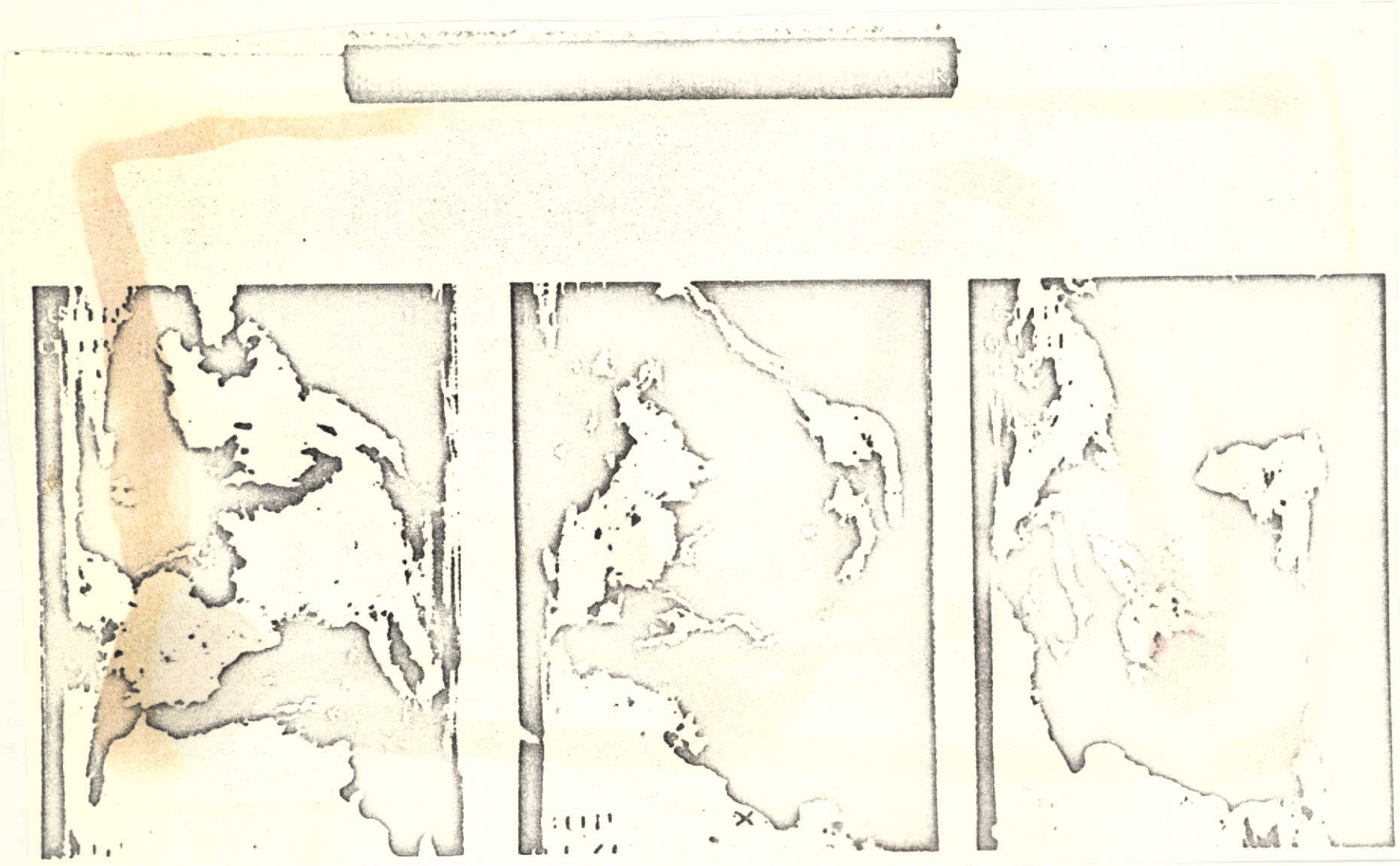

Figs. 3.2-3.4. HRIR -- photos of Nimbus III of May 26, 1969, May 27, 1969, and May 28, 1969 (left to right).

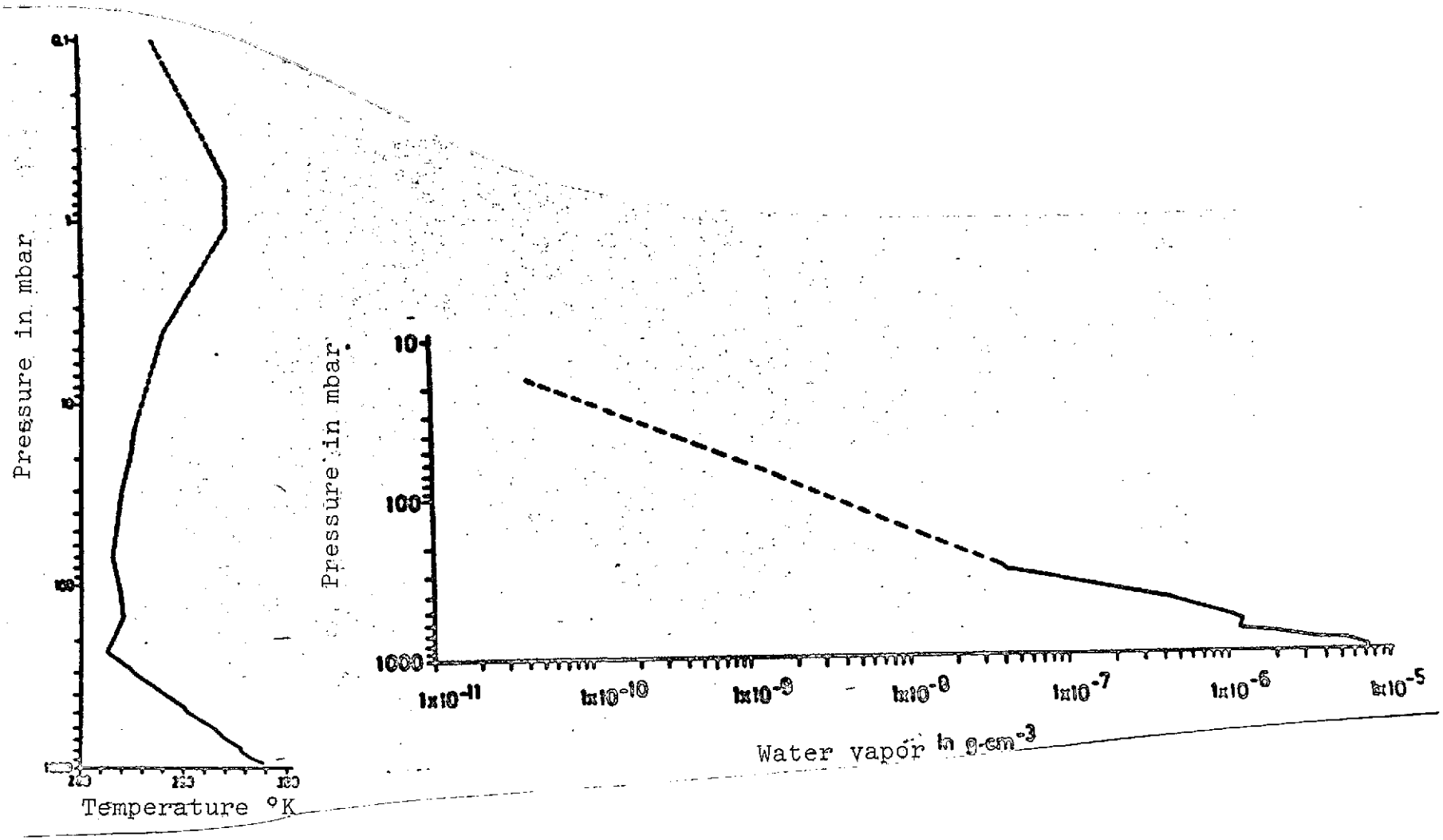

Fig. 4.1. Temperature and water vapor distribution of the Munich Riem radio-probe on May 27, 1969, 12:00 GMT.
(---- Values extrapolated according to [4]).

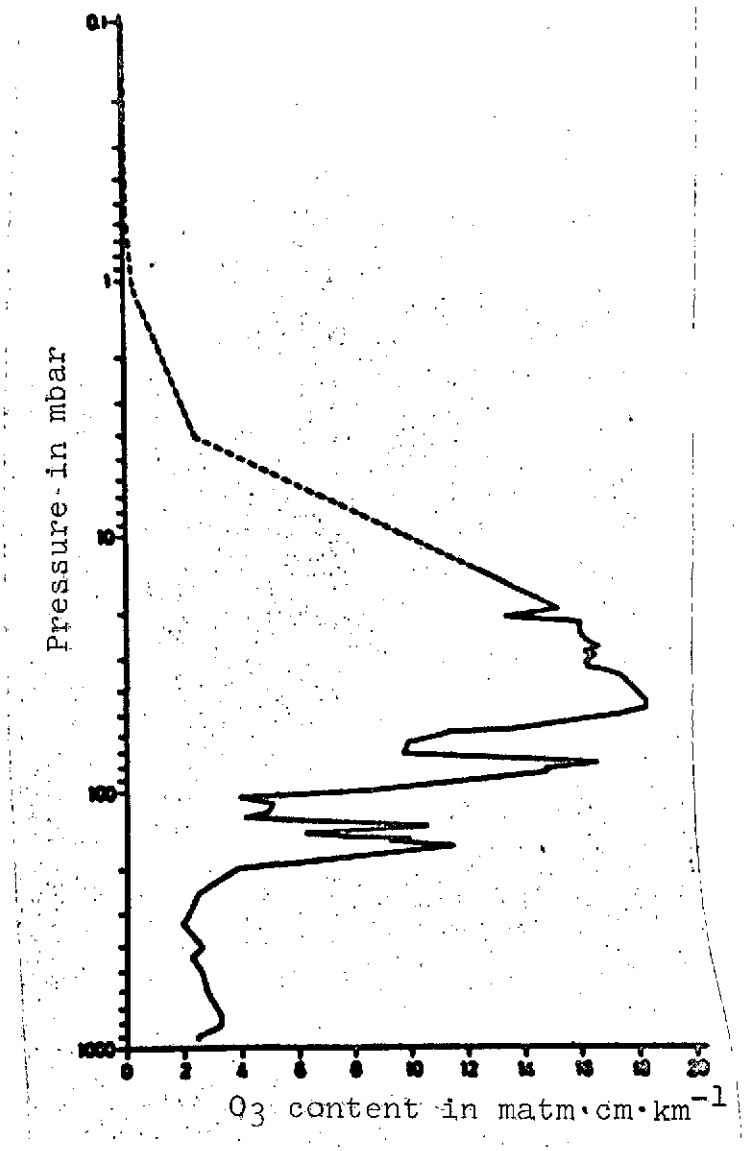

Fig. 4.2. Ozone distribution for Hohenpeissenberg on May 27, 1969, 7:41 CET [Central European Time]. (---- Values extrapolated according to [4]).

/37

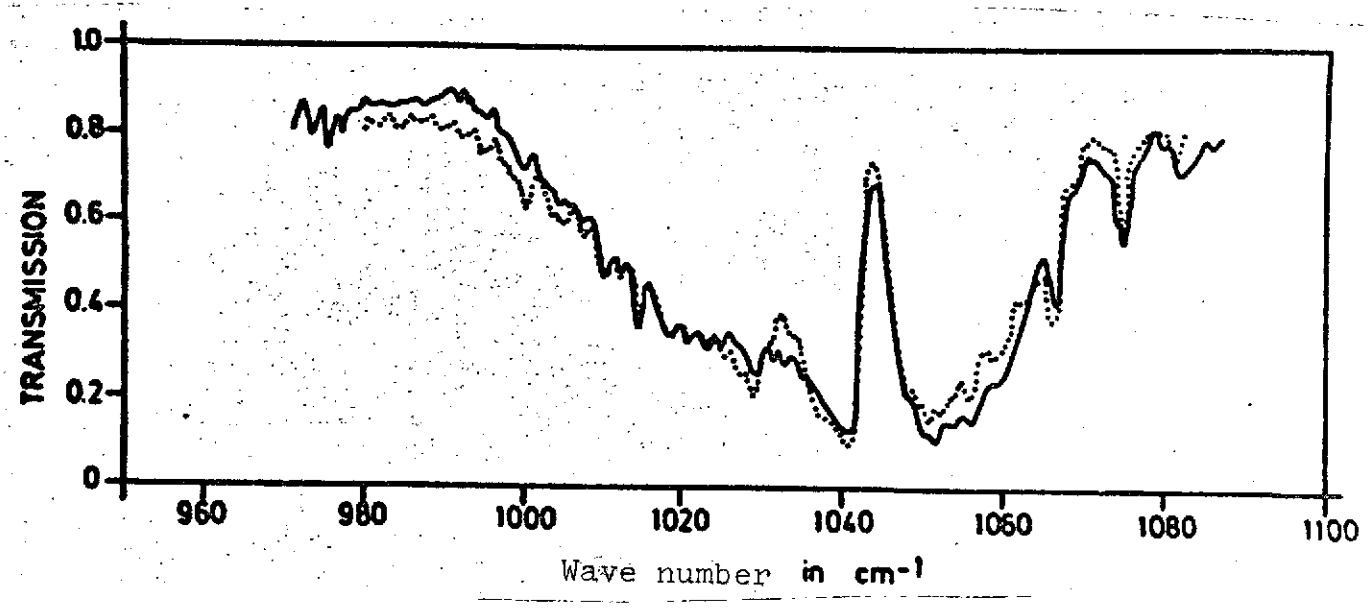

Fig. 6.1. Measured transmission spectrum and transmission spectrum calculated with corrected line data at Maisach on May 27, 1969, 9:41 CET $(O_3 + H_2O + CO_2)\cdot\zeta = 39.82°$.
——— Measured ····· Calculated

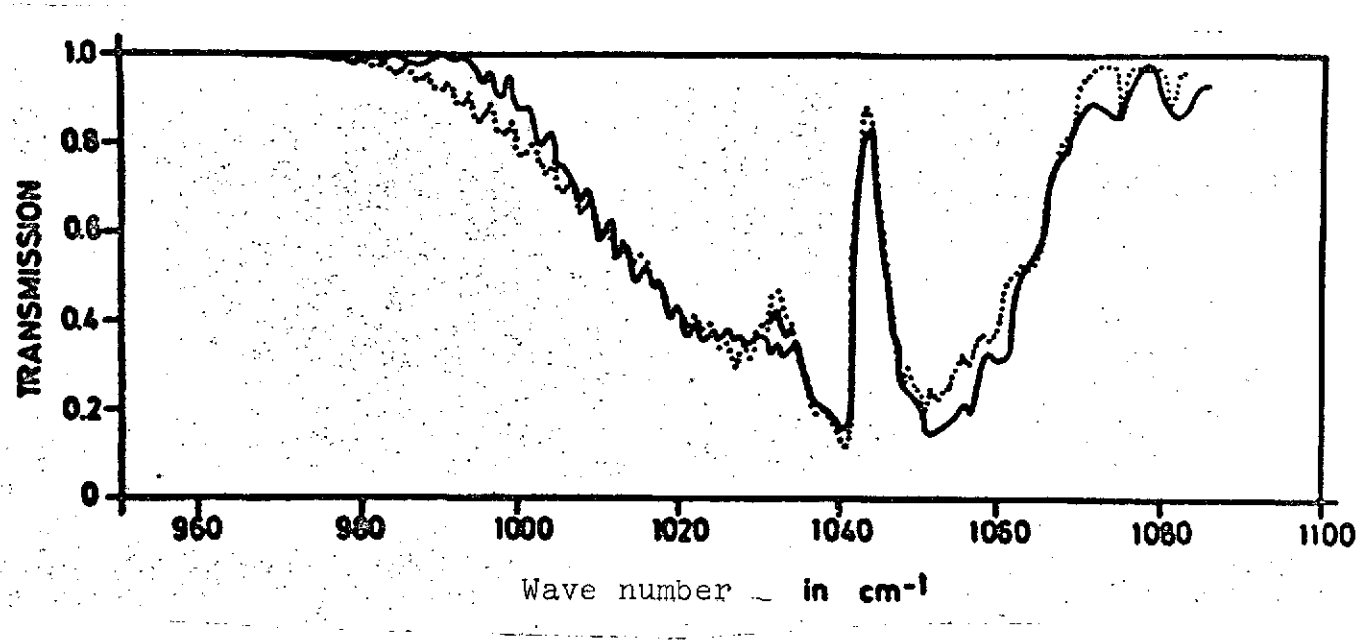

Fig. 6.2. Measured transmission spectrum and transmission spectrum calculated with corrected line data at Maisach on May 27, 1969, 9:41 CET.
$(O_3) \cdot \zeta = 39.82°$.
Transmissions (O_3) calculated with the aid of new line data
——— Measured ..... Calculated ▬▬ Calculated with new line data.

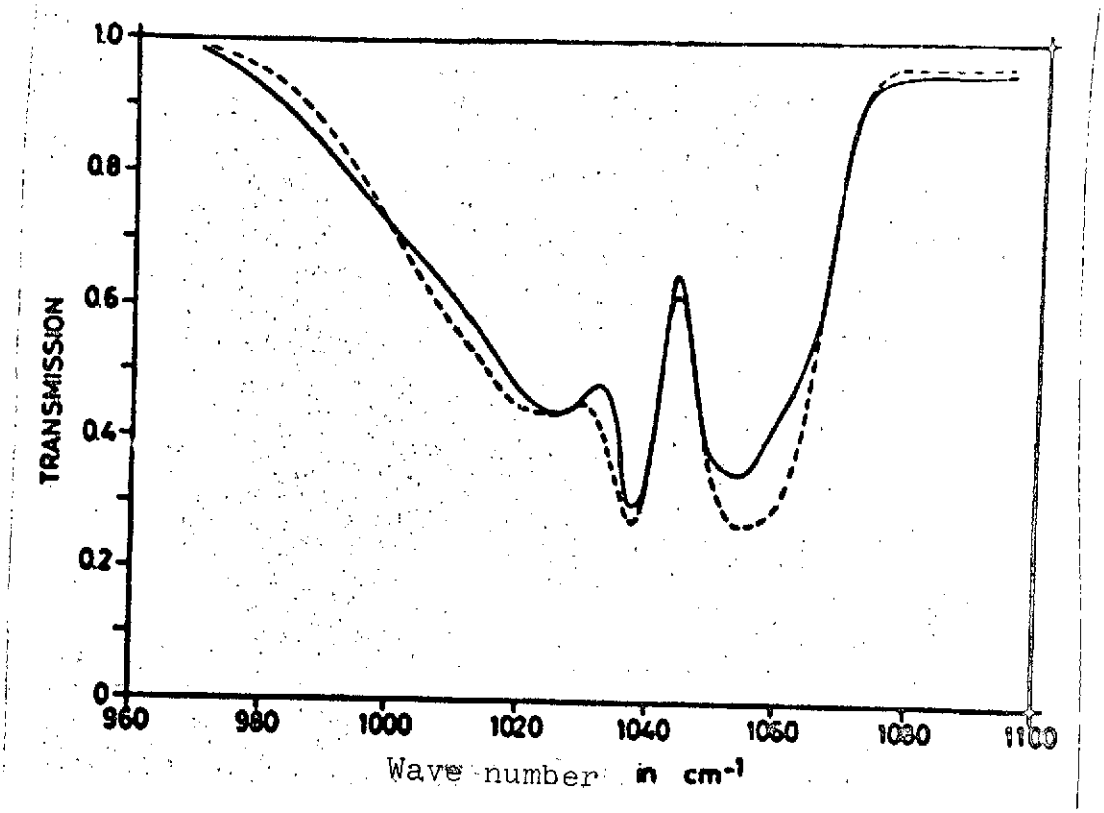

Fig. 6.3. Spectra calculated with corrected and new line data. /40
(m_{O_3} = 0.41 atm-cm, p = 66.6 mbar, T = 296°K).

——— Corrected line data
----- New line data

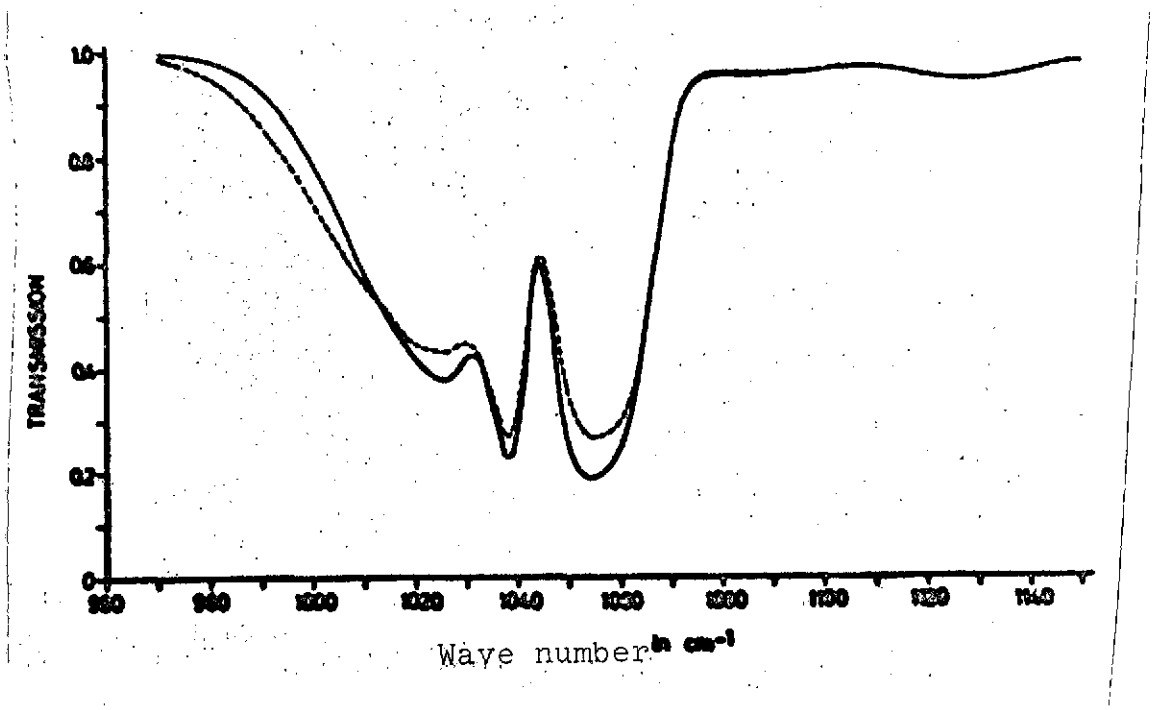

Fig. 6.4. Spectra calculated with uncorrected and with new line data.
(m_{O_3} = 0.41 atm-cm, p = 66.6 mbar, T = 296.2°K). /41

——— Uncorrected line data
----- New line data

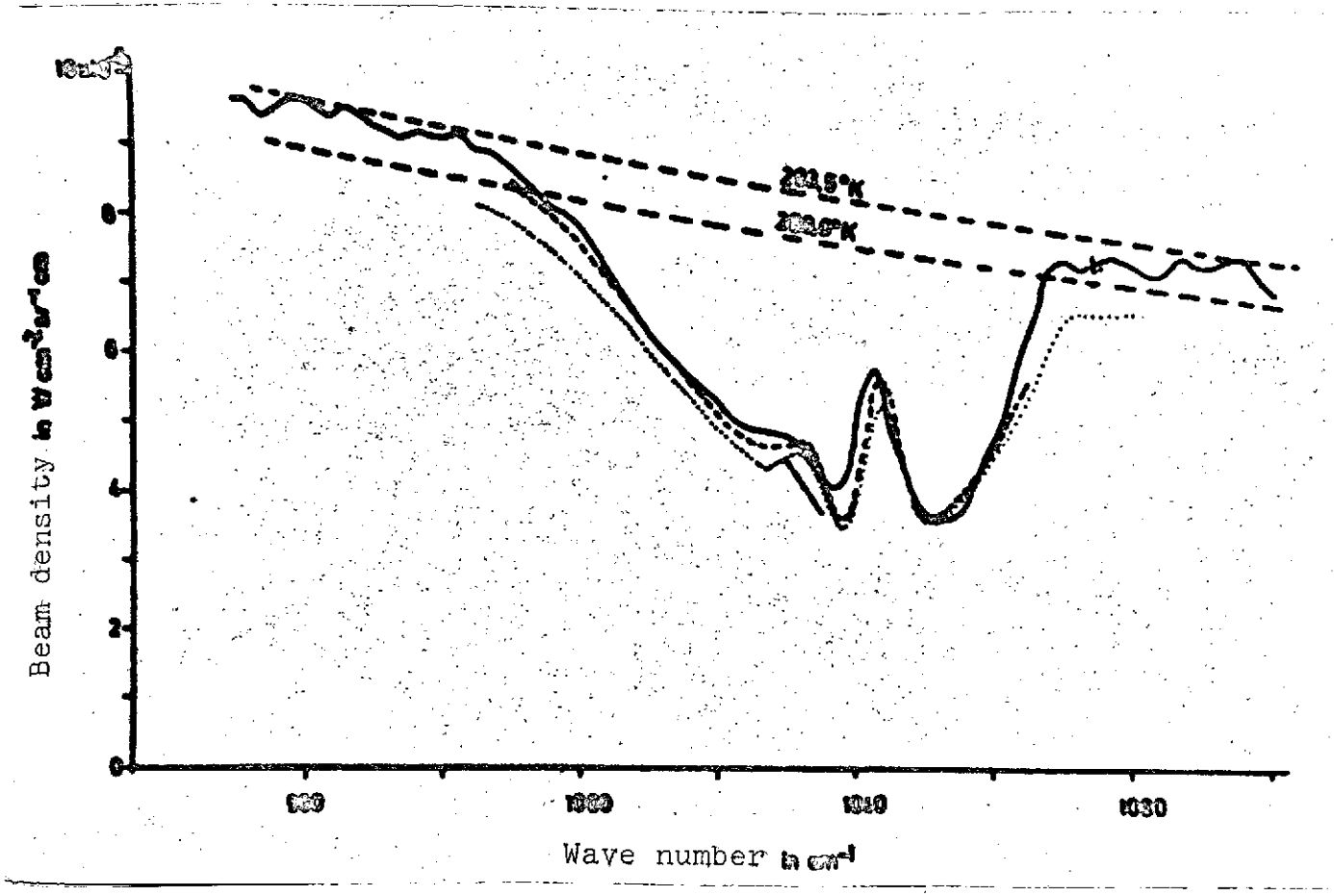

Fig. 6.5. Emission spectrum of Nimbus III on May 27, 1969, 10:03 GMT.

——— Measured spectrum (T_{ground} = 293.5°K),
..... Calculated spectrum (T_{ground} = 289°K)
-·-·- Spectral range (T_{ground} = 289°K) estimated for new line data
----- Calculated spectrum estimated for T_{ground} = 293.5°K

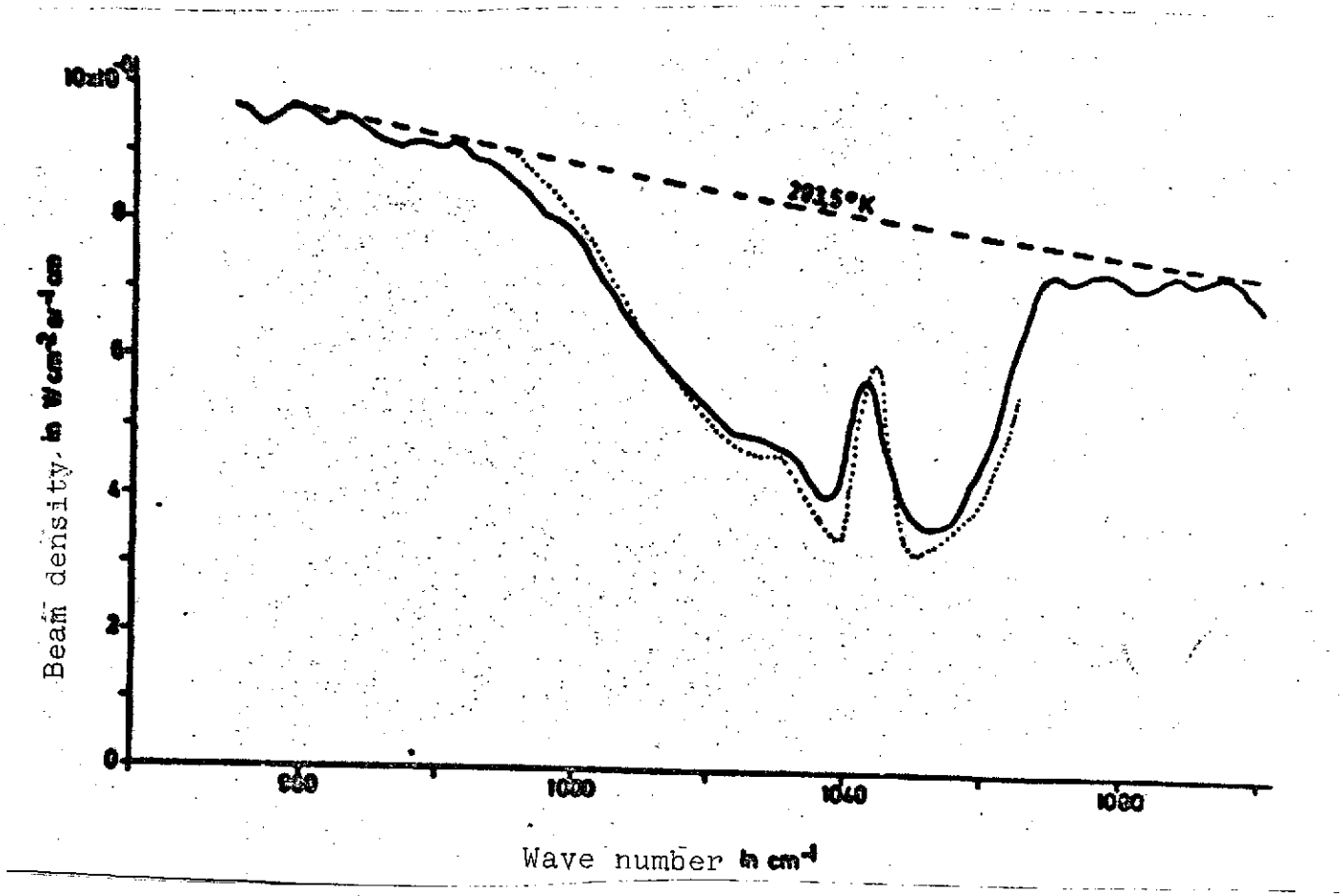

Fig. 6.6. Emission spectrum of Nimbus III of May 27, 1969, 10:03 GMT with T_{ground} = 293.5°K.

——— Measured spectrum
..... Calculated spectrum, estimated for new line data

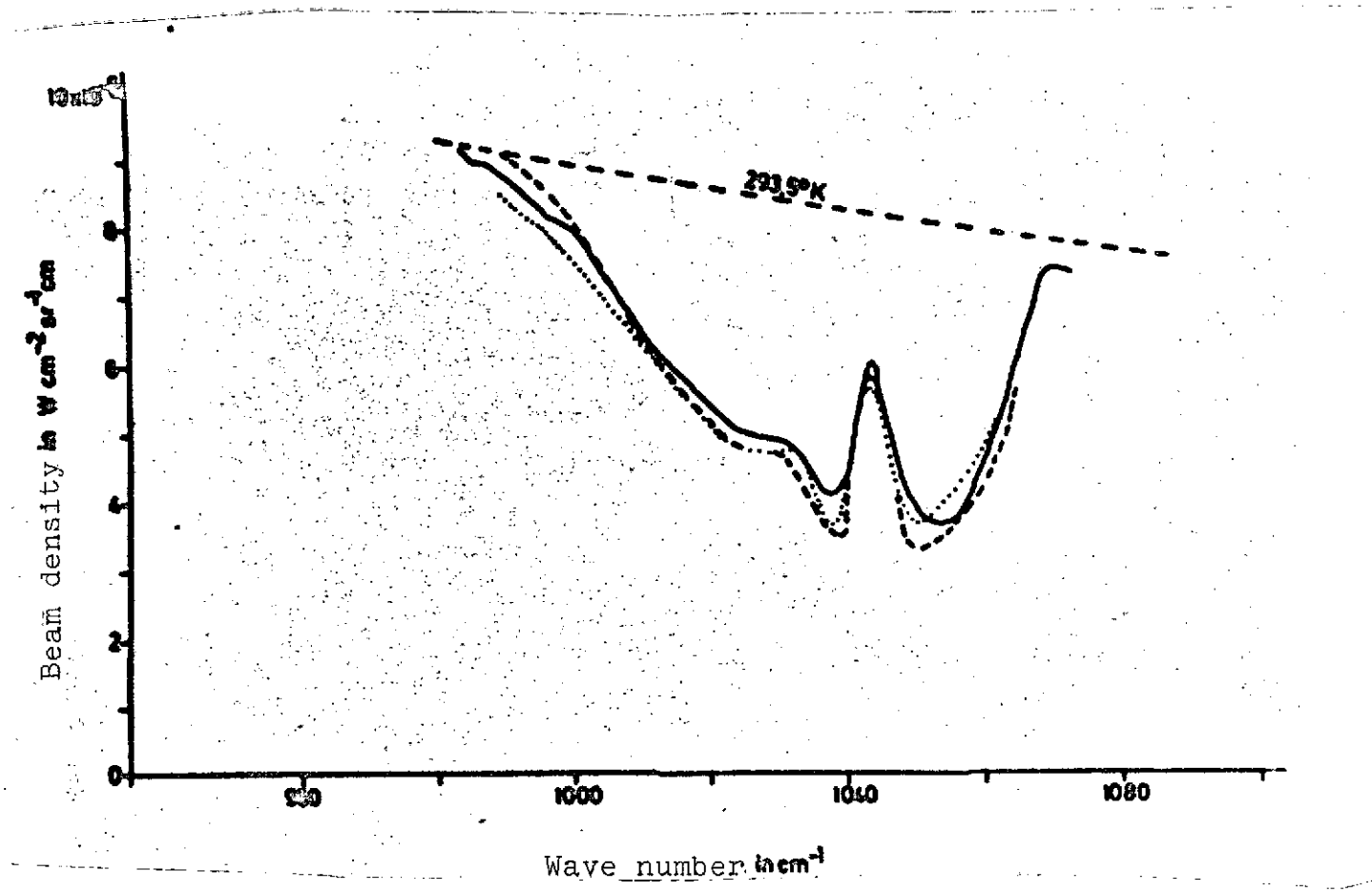

Fig. 6.7. Emission spectra of Nimbus III of May 27, 1969, 10:03 GMT with T_{ground} = 293.5°K without shift in wave number.

——— Measured ..... Calculated with corrected line data
----- Estimated for new line data

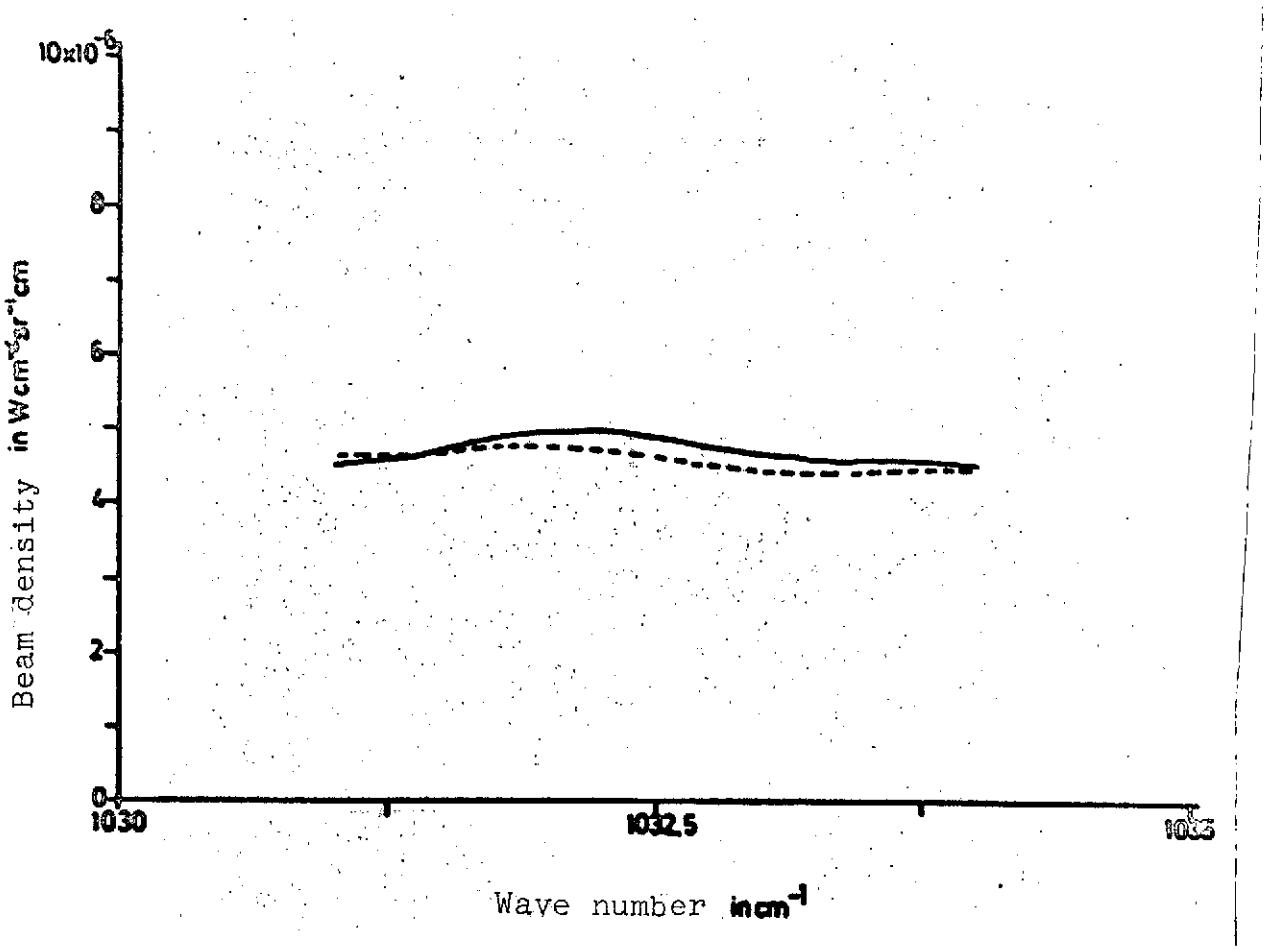

Fig. 6.8. Atmospheric emission spectra calculated with new and old line data for May 27, 1969, 10:03 GMT. (Resolution 1 cm^{-1}, T_{ground} = 289°K).

——— Old line data ----- New line data

/45

REFERENCES

1. Armstrong, B. H., "Spectrum line profiles: the Voigt function," J. Quant. Spectrosc. Radiat. Transfer 7, 1967. /32

2. Attmannspacher, W., private communication.

3. Benedick, W. S. and Kaplan, L. D., J. Chem. Phys., 30, 388 (1959).

4. Bolle, H.-J., "Infrared spectroscopy as an aid and subject of meteorological planetary research," Research Report No. W67-17, Meteorological Institute, Munich, 1967.

5. Bolle, H.-J., "Investigations of the atmospheric infrared radiation in the Gulf of Naples," Geofis. Pura. Appl. 53, 159-170 (1962).

6. Carlon, H. R., "Infrared emission by fine water aerosols and fogs," Appl. Opt. 9, 200 (1970).

7. Clough, A. and Kneizys, F. X., "Ozone absorption in the 9.0 micron region," Physical Sciences Research Papers, No. 170, AFCRL-65-862, 1965.

8. Dütsch, H. U., private communication, 1970.

9. Farmer, C. B. and Key, P. J., "A study of the solar spectrum from 7 μ to 400 μ," Appl. Opt. 4, 1051 (1965).

10. Goldman, A., Kyle, T. G., Murcray, D. G., Murcray, F. H., and Williams, W. J., "Long path atmospheric ozone absorption in the 9-10 μ region observed from a balloon-borne spectrometer," Appl. Opt. 9, 565 (1970).

11. Goldman, A., and Kyle, T. G., "A comparison between statistical model and line by line calculation with application to the 9.6 μ ozone and the 2.7 μ water vapor bands," Appl. Opt. 7, 1167 (1968).

12. Goldman, A., "Statistical band model parameters for long path atmospheric ozone in the 9-10 μ region," Appl. Opt. 9, 2600 (1970).

13. Grassl, H., Wendling, P., and Bolle, H.-J., "Preparation of a method for the prediction of thermal radiation, infrared transmission of clouds," Report No. VIII, Research Contract No. T 741-I-203 of the Federal Minister of Defense (TII3), 1969.

14. Hanel, R., and Conrath, B., "Preliminary Results from the Interferometer experiment on Nimbus III," NASA, Goddard Space Flight Center, Greenbelt.

15. Kunde, V. G., "Theoretical computations of the outgoing infrared radiance from a planetary atmosphere," NASA Report TN D-4045, 1967, p. 19.

16. Labs, D., and Neckel, H., "The radiation of the solar photosphere from 2000 A to 100 μ," Z. Astroph. 69, 1-73 (1968).

17. McCaa, D. J., and Shaw, J. H., "The infrared absorption bands of ozone," Scientific Report No. 2, ARCRL-67-0237, Contract No. AF 19(628)-3806, Ohio State University, 1956.

18. Selby, J. E. A., and McClatchey, R. A., Air Force Cambridge Research Laboratories USA, 1970.

19. Migeotte, M., Neven, L., and Swensson, J., "The solar spectrum from 2.8 to 23.7 μ," Institut D'Astrophysique de L'Universite de Liege, Observatoire Royal de Belgique, Special Vol. No. 1 and 2, 1956.

20. The Nimbus III User's Guide, Goddard Space Flight Center.

21. The Nimbus III Data Catalog, Vol. 1, Part 1-3, Goddard Space Flight Center, Greenbelt, Maryland.

22. Prabhakara, C., Conrath, B. J., and Hanel, R. A., "Remote sensing of atmospheric ozone using the 9.6 μ band," Goddard Space Flight Center, Greenbelt.

23. Quenzel, H., Tabellen der Sonnenstände und Luftmassen von Maisach, [Tables of Sun Positions and Air Masses at Maisach].

24. Rest, R., Korrekturverfahren für die Linienintensitäten der 9.6 μ-bande des Ozons, [Corrections Methods for Line Intensities of the 9.6 μm Bands of Ozone], Munich University, 1968.

25. Saiedy, F., and Goody, R. M., "Solar emission intensity at 11 μ," Mon. Notic. Roy. Astron. Soc. 119, 213 (1959).

26. "Special observations of the Hohenpeissenberg Meterological Observatory," No. 8, 1969.

27. Volz, F. E., Ann. Meterol. 8, 34 (1957).

APPENDIX

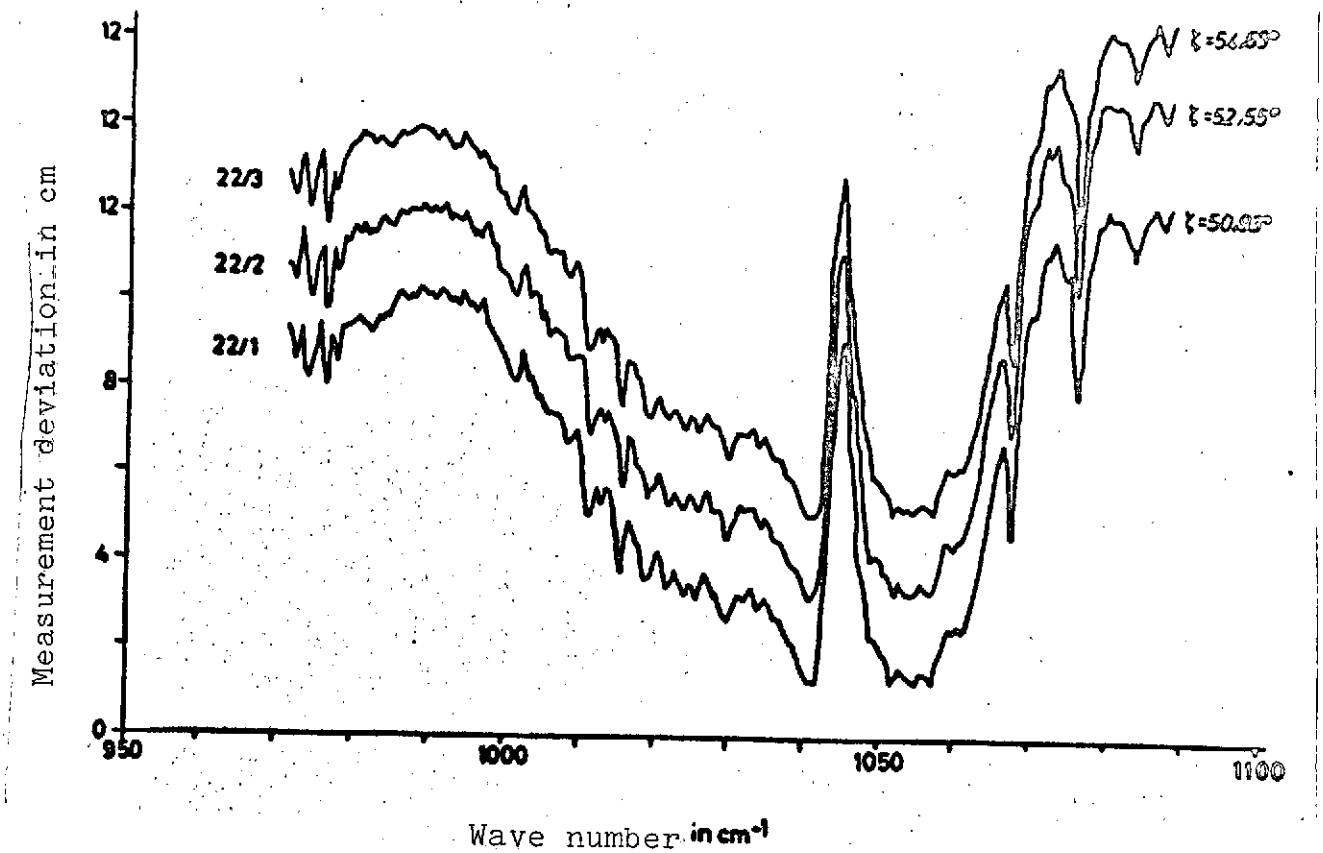

Fig. 1. Transmission spectra at Maisach on May 22, 1969. The spectra have been shifted in each case by a 2 cm measurement deviation. All spectra have been corrected by means of a permeability curve of the spectrograph. /47

No.	Time (CET)	Air temperature (°C)	Ground pressure mbar	Water vapor (gcm^{-3})
22/1	15:46	19	962	$0.695 \cdot 10^{-5}$
22/2	15:56	19	962	0.695
22/3	16:09	19	962	0.695

(ζ: Zenith angle)

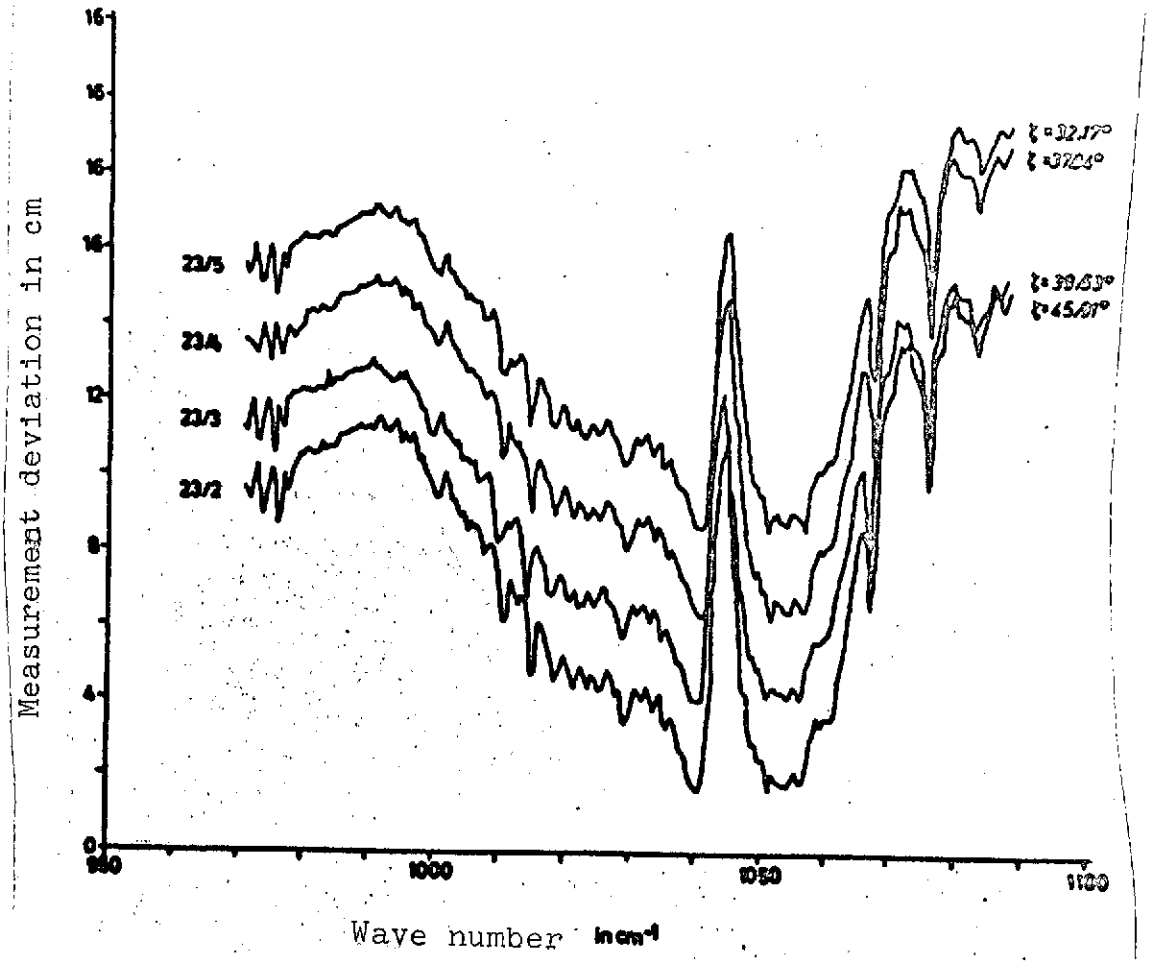

Fig. 2. Transmission spectra at Maisach on May 23, 1969. The spectra have been shifted in each case by a 2 cm measurement deviation. All spectra have been corrected by means of a permeability curve of the spectrograph.

/48

No.	Time (CET)	Air temperature (°C)	Ground pressure mbar	Water vapor (gcm^{-3})
23/2	9:08	18.0	955	$0.900 \cdot 10^{-5}$
23/3	9:50	18.0	955	0.905
23/4	10:02	18.0	955	0.905
23/5	10:50	18.5	955	0.913

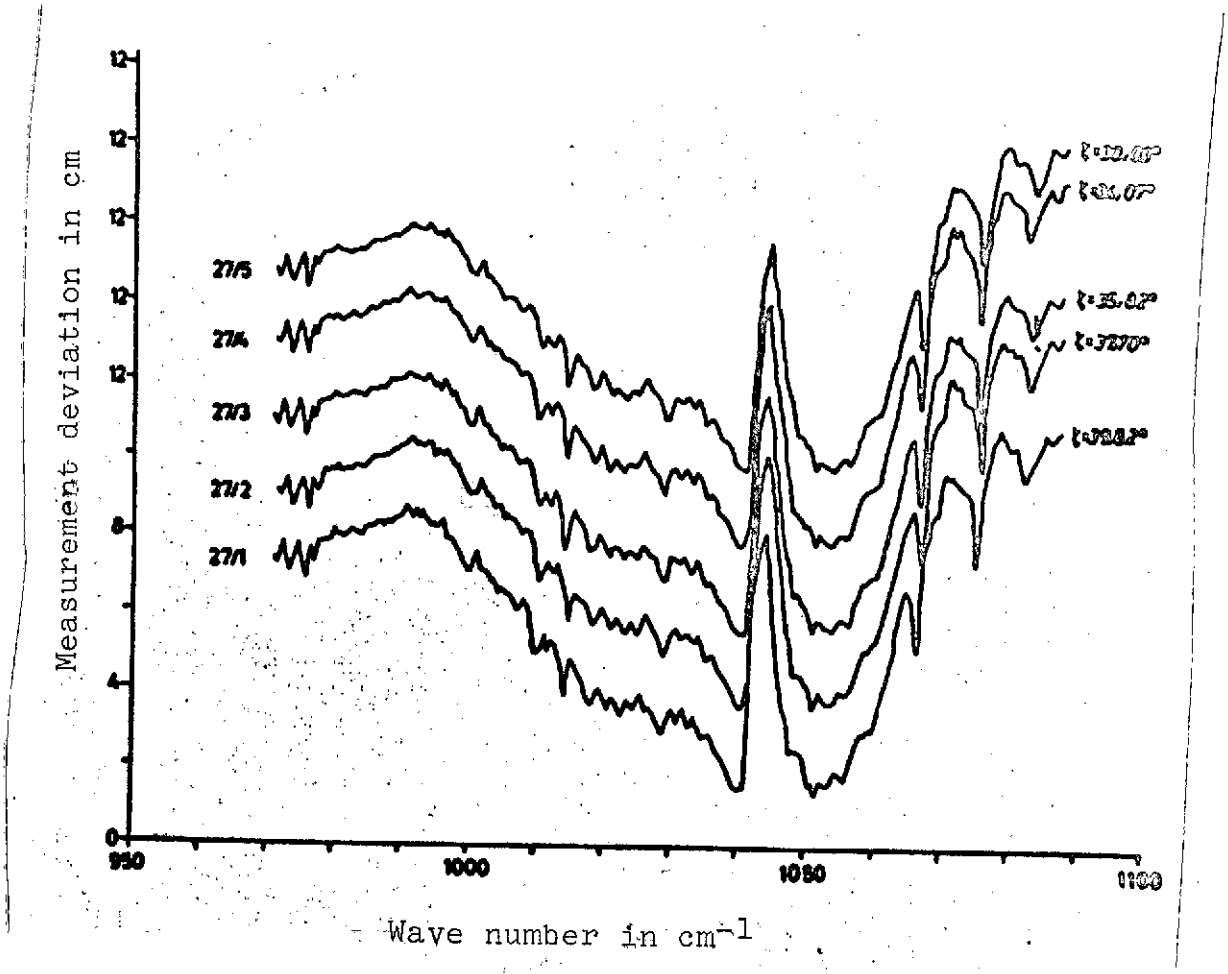

Fig. 3a. Transmission spectra at Maisach on May 27, 1969. The spectra have been shifted in each case by a 2 cm measurement deviation. All spectra have been corrected by means of a permeability curve of the spectrograph. /49

No.	Time (CET)	Air temperature (°C)	Ground pressure mbar	Water vapor (gcm^{-3})
27/1	9:45	16.0	954	$0.745 \cdot 10^{-5}$
27/2	10:00	16.0	954	0.745
27/3	10:14	16.0	945	0.745
27/4	10:27	16.0	945	0.745
27/5	11:06	16.5	945	0.770

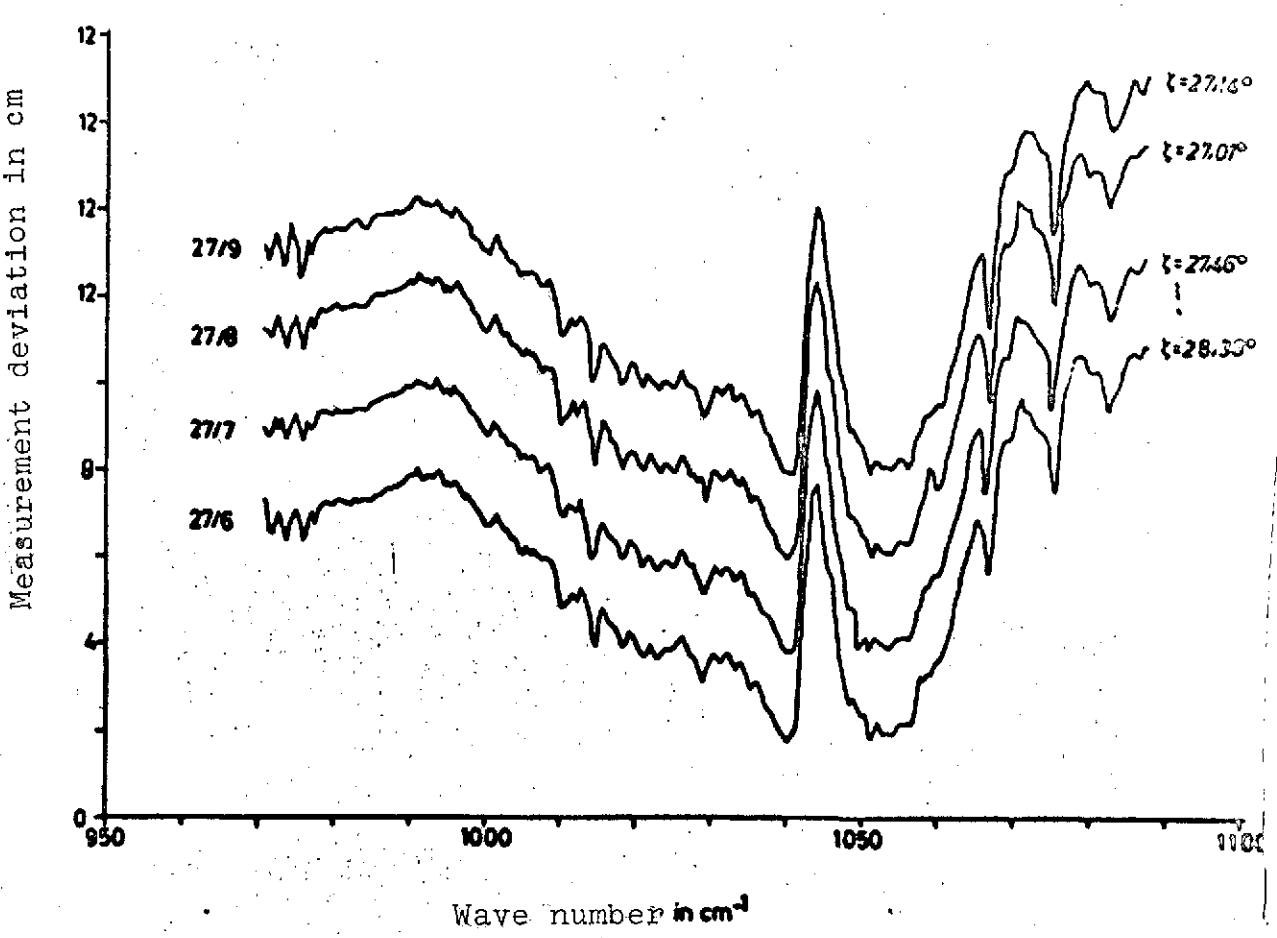

Fig. 3b. Transmission spectra at Maisach on May 27, 1969. The spectra have been shifted in each case by a 2 cm measurement deviation. All spectra have been corrected by means of a permeability curve of the spectrograph.

/50

No.	Time (CET)	Air temperature (°C)	Ground pressure mbar	Water vapor (gcm^{-3})
27/6	11:31	16.8	954	$0.775 \cdot 10^{-5}$
27/7	11:46	17.0	954	0.775
27/8	12:04	17.0	954	0.775
27/9	12:28	17.0	954	0.775

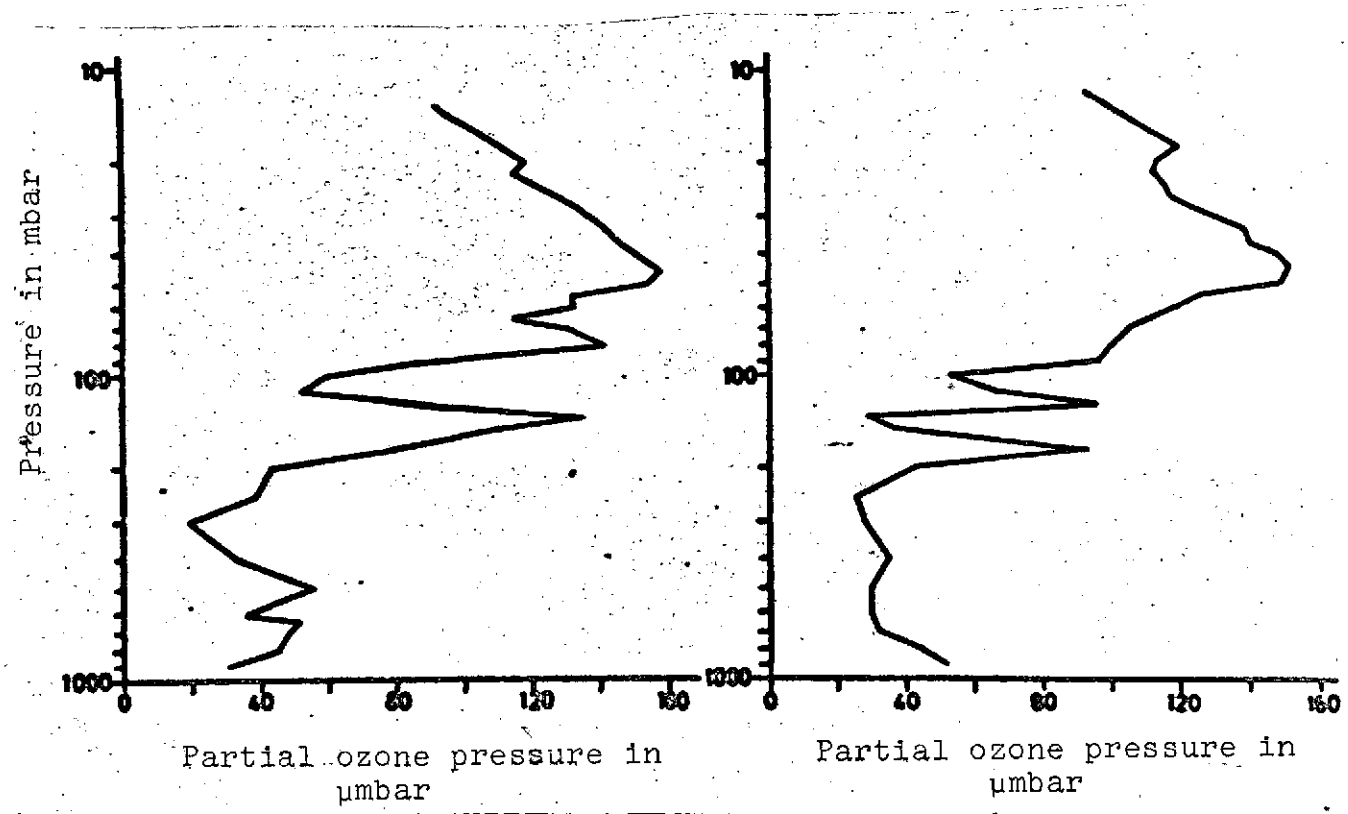

Fig. 4. Ozone profile at Hohenpeissenberg on May 21, 1969. Total ozone 364.0 matm-cm

Ozone profile at Payerne on May 21, 1969. Total ozone 349.0 matm-cm.